

## Disclination loop behavior near the nematic-isotropic transition

N. V. Priezjev and Robert A. Pelcovits

*Department of Physics, Brown University, Providence, Rhode Island 02912*

(Received 23 May 2001; published 29 August 2001)

We investigate the behavior of disclination loops in the vicinity of the first-order nematic-isotropic transition in the Lebwohl-Lasher and related models. We find that two independent measures of the transition temperature, the free energy, and the distribution of disclination line segments, give essentially identical values. We also calculate the distribution function  $D(p)$  of disclination loops of perimeter  $p$  and fit it to a quasiexponential form. Below the transition,  $D(p)$  falls off exponentially, while in the neighborhood of the transition, it decays with a power-law exponent approximately equal to 2.5, consistent with a “blowout” of loops at the transition. In a modified Lebwohl-Lasher model with a strongly first-order transition we are able to measure a jump in the disclination line tension at the transition, which is too small to be measured in the Lebwohl-Lasher model. We also measure the monopole charge of the disclination loops and find that in both the original and modified Lebwohl-Lasher models, there are large loops that carry monopole charge, while smaller isolated loops do not. Overall, the nature of the topological defects in both models is very similar.

DOI: 10.1103/PhysRevE.64.031710

PACS number(s): 64.70.Md, 61.30.Jf

### I. INTRODUCTION

In many physical systems, particularly two-dimensional ones with continuous order parameter symmetry, topological defects can play an essential role at the phase transition between the ordered (or quasicrystalline) and disordered phases. Using simple physical arguments Kosterlitz and Thouless [1] pointed out that phase transitions in two-dimensional superfluid  $^4\text{He}$ , crystalline solids, and  $XY$  magnets would occur via the unbinding of point topological defects. Subsequently, Kosterlitz [2] developed a renormalization-group theory for the two-dimensional  $XY$  model that provided quantitative predictions for this defect-mediated critical behavior. Renormalization-group theories for the defect-mediated melting of crystalline solids in two dimensions were developed by Nelson and Halperin [3] and Young [4].

The theoretical picture for defect-mediated phase transitions in three dimensions is less clear. It is expected on the basis of the Villain representation [5] that the transition in the three-dimensional  $XY$  model is mediated by vortex loops [6]. In this scenario, there is a finite length scale at low temperatures associated with the typical size of vortex loops that disorder the system on smaller length scales. At the phase transition, loops can exist on all length scales, i.e., there is “vortex-loop blowout” [7,8] and the system enters the disordered phase. Scaling and renormalization-group theories have been developed [9] that provide quantitative predictions for the critical behavior, though these theories are not as well established as the corresponding Kosterlitz-Thouless theory in two dimensions. Monte Carlo simulations [10,11] have yielded further support for this vortex loop picture of the phase transition. In the three-dimensional Heisenberg model, there is also numerical evidence [12] for a phase transition mediated by point topological defects (monopoles), though this evidence has been questioned by other authors [13].

The role of topological defects at the nematic-isotropic phase transition poses intriguing questions. The defect structure in nematics is particularly rich and while sharing some similarities with the defect structures of the  $XY$  and Heisenberg models, there are significant differences due to the na-

ture of the order-parameter space. The local director  $\hat{\mathbf{n}}$  of a nematic liquid crystal is defined as the average direction of alignment of a group of molecules. However, unlike the case of ferromagnets, the directions  $\hat{\mathbf{n}}$  and  $-\hat{\mathbf{n}}$  are equivalent. Thus, the order-parameter space for nematics is  $P_2$ , the unit sphere with antipodal points identified. The stable topological defects [14] include monopoles and disclination lines. The monopoles are similar to the point defects of the Heisenberg model, though in the latter case, positive and negative topological charges of the same absolute value are distinct, whereas they are equivalent in the nematic [15]. While defect lines in the  $XY$  model can have any integer value with either positive or negative sign, one value of topological charge,  $+1/2$ , characterizes the entire class of stable line defects in nematics [15,16]. All other half-integer valued lines, whether positive or negative, can be continuously deformed to a line with charge  $+1/2$ , and integer-valued lines can “escape in the third dimension” [17]. As in the  $XY$  model, the disclination lines form closed loops or terminate on the surface of the sample because of the prohibitive energy cost of a free line end. However, whereas the  $XY$  model loops carry no net monopole charge, nematic disclination loops *can* (though all need not) carry monopole charge [18].

Not only is the classification of defects different in the nematic compared with the  $XY$  and Heisenberg models, but also the nature of the phase transition, first order in the former case and continuous in the latter. Lammert *et al.* [19] have argued that disclination lines are responsible for the first-order nature of the nematic-isotropic (NI) transition. They developed and studied a lattice model of liquid crystals that allows for the suppression of the line defects while maintaining the presence of monopoles as in the Heisenberg model. As the defect lines are made more costly, Lammert *et al.* found that the transition between the ordered nematic phase (characterized by a nonzero disclination line tension) and the isotropic phase (characterized by zero line tension) becomes more weakly first order. At sufficiently large values of the core energy, the transition splits into a pair of continu-

ous transitions, and a new phase appears with no long-range nematic order but nonzero disclination line tension. In the extreme limit where the disclination lines are completely suppressed, their model reduces to the Heisenberg model with the expected continuous phase transition.

In this paper, we report on a numerical study of topological defect behavior near the NI transition in the Lebwohl-Lasher (LL) lattice model [20] of liquid crystals that exhibits a weakly first-order phase transition (a weak first-order transition is characteristic of real experimental systems as well). We also consider the defect behavior in a modified LL model that exhibits a strongly first-order transition. We find that two independent measures of the NI transition temperature, one the free energy and the other the distribution of disclination line segments, give almost identical values. By measuring the distribution of disclination loops as a function of their perimeter, we find evidence for the “blowout” of disclination loops at the transition, similar to the three-dimensional  $XY$  model. The disclination line tension in the modified LL model drops discontinuously to zero at the transition; in the case of the LL model, the transition is too weakly first order to detect a similar discontinuity. We also measure the monopole charge of the loops and find in both the LL model and its modification that large loops and small loops adjacent to large loops have nonzero monopole charge, while small isolated loops do not. There appear to be no significant differences between the two models in the nature of the topological defects present.

In Sec. II we provide the details of our simulations and results, followed in Sec. III by our conclusions.

## II. SIMULATIONS AND RESULTS

We performed Monte Carlo simulations on the Lebwohl-Lasher model, a lattice model of rotors with an orientational order-disorder transition. While it neglects the coupling between the orientational and translational degrees of freedom present in a real nematic liquid crystal, it is generally believed that this coupling does not play a significant role at the NI transition. With the absence of translational degrees of freedom, the LL model is particularly well suited for large-scale simulations of the transition. The model is defined by the Hamiltonian

$$\mathcal{H}_{LL} = -J \sum_{\langle ij \rangle} P_2(\sigma_i \cdot \sigma_j) = -J \sum_{\langle ij \rangle} \left\{ \frac{3}{2} (\sigma_i \cdot \sigma_j)^2 - \frac{1}{2} \right\}, \quad (1)$$

where the sum is over all nearest-neighbors rotors situated on a cubic lattice. The long axes of the rotors are specified by the unit vectors  $\sigma_i$ ,  $P_2$  is the second-order Legendre polynomial, and  $J$  is a coupling parameter. The LL model has been intensively investigated using Monte Carlo techniques since its introduction [21–27,35]. The most complete numerical analysis of the NI transition in the LL model using the conventional single spin-flip Metropolis algorithm was carried out by Zhang *et al.* [26] on systems up to a size of  $28^3$ . However, the single spin-flip algorithm is inefficient in the critical region and during the course of a simulation, the

system becomes trapped in one of the local minima corresponding to either the ordered or disordered phases. This difficulty can be overcome by using a cluster algorithm that is most efficient in the critical region and the system samples both local minima effectively. The first such algorithm for nematic liquid crystals was introduced by Kunz and Zumbach [28] to study the two-dimensional LL model. Their algorithm is a modification of the Wolff algorithm [29] for ferromagnetic systems, and greatly reduces critical slowing down. In an earlier publication [30], we used the Kunz-Zumbach algorithm to carry out a finite-size scaling analysis of the NI transition in the three-dimensional LL model with systems sizes up to  $70^3$  using the Ferrenberg-Swendsen reweighting technique [31].

Here we use the cluster algorithm to study the behavior of disclination lines and monopoles in the critical region. Following Ref. [19], we introduce a disclination line segment counting operator,

$$D_{ijkl} \equiv \frac{1}{2} [1 - \text{sgn}\{(\sigma_i \cdot \sigma_j)(\sigma_j \cdot \sigma_k)(\sigma_k \cdot \sigma_l)(\sigma_l \cdot \sigma_i)\}], \quad (2)$$

which is unity if a disclination line segment pierces the lattice square defined by the four rotors  $\sigma_i$ ,  $\sigma_j$ ,  $\sigma_k$ , and  $\sigma_l$ . This method of locating disclination segments is mathematically equivalent to the method of Zapotocky *et al.* [32]. A disclination line segment can be considered as a bond on a cubic lattice dual to the original lattice of the rotors, and only an even number of bonds meet at a dual lattice site. Connecting the bonds to form disclination loops cannot be done in a unique way when four or six bonds meet at a site. To deal with this ambiguous case we followed the approach of Ref. [11] and chose a random pairing of the bonds. We thus traced the path of each disclination line through the system until the path crossed itself and formed a loop. The bonds of the loop were then eliminated from the dual lattice to avoid double counting when additional loops were traced.

We considered several measures of the nature of the disclination segments and loops, including the number of segments in the nematic and isotropic phases at coexistence, the distribution of loops as a function of their perimeter, and the monopole charge of the loops.

We simulated a system of size  $70^3$  (with periodic boundary conditions) for  $5 \times 10^6$  Monte Carlo steps (MCS) where one MCS corresponds to one cluster formation attempt and update of the spins comprising the cluster. Every 200 MCS, we measured the total number of disclination line segments in the system and stored our data in a histogram. The logarithm of this histogram is shown in Fig. 1 at the temperature  $T = 1.1226$  (temperatures measured in units of  $J/k_B$ ) where the two wells have equal depth. The right-hand well corresponds to the isotropic phase (which we confirm by monitoring the nematic order parameter) and the left-hand well with fewer disclination line segments corresponds to the nematic phase. Varying the temperature by as little as 0.0001 yields wells of unequal depths. In our earlier work [30], we used the cluster algorithm to compute a histogram of the free energy (as a function of  $E = \mathcal{H}_{LL}/N$ , the energy per site). We

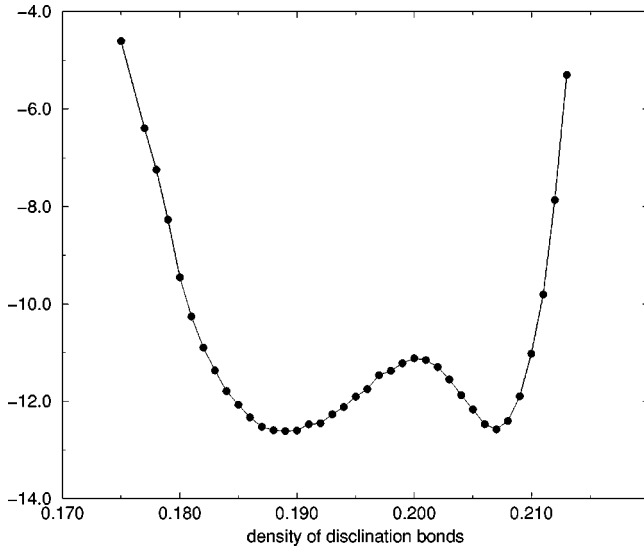


FIG. 1. The logarithm of the distribution of disclination bond density in the Lebwohl-Lasher model, Eq. (1) for system size  $70^3$  at the NI transition temperature  $T_{NI}=1.1226$ . The density is defined as the ratio of the number of disclination bonds to the total number of lattice bonds ( $3 \times 70^3$  in the present case). The solid line is a guide to the eye.

found a double-well structure for the free energy with equal well depths occurring at the temperature  $T=1.1226$ , which we then identified as  $T_{NI}$ . Thus, the appearance of equal-well depths in the histogram for the density of disclination line segments at the *same* temperature (to within our numerical accuracy) suggests that disclinations play a crucial role at the NI transition.

To further assess the role played by disclination loops at the transition, we followed the approach used in Ref. [11] to study defect behavior at the three-dimensional  $XY$  transition, and calculated the perimeter distribution function  $D(p)$  (the average number of loops with perimeter  $p$ ). In Refs. [11]  $D(p)$  was fit to the following form:

$$D(p) = Ap^{-\alpha} \exp[-\epsilon(T)p/k_B T], \quad (3)$$

where  $\epsilon(T)$  is the effective vortex line tension which is non-zero at low temperatures. Thus, in the low-temperature ordered-phase vortex loops with large  $p$  are exponentially suppressed, and the length scale  $L_0$  governing the typical perimeter size of the vortex loops is given by  $L_0 = k_B T / \epsilon(T)$ . At the critical temperature  $T_c$  of the  $XY$  model,  $\epsilon(T)$  vanishes continuously and the distribution  $D(p)$  has a power-law form. Consequently there will be a finite probability of having vortex loops that traverse the entire system and destroy the long-range order.

We computed  $D(p)$  at the NI transition temperature  $T_{NI}=1.1226$  (identified by the two methods described above) and at two slightly lower temperatures. The results are shown in Fig. 2. We simulated the system for  $5 \times 10^6$  MCS and computed  $D(p)$  every 200 MCS to make sure that the successive configurations for bonds distribution are completely updated. Fitting our data to the form Eq. (2) yields  $\alpha = 2.50 \pm 0.05$ . For noninteracting loops (i.e., random walks)

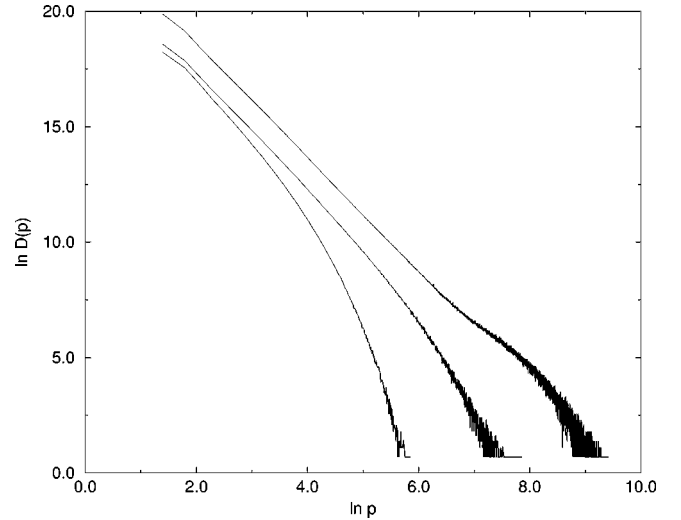


FIG. 2. Log-log plot of the disclination loop distribution function  $D(p)$  [Eq. (3)] in the Lebwohl-Lasher model, Eq. (1) for system size  $70^3$  at temperatures:  $T_c=1.1226$  (top curve),  $T=1.120$  (middle curve), and  $T=1.10$  (bottom curve).

we expect  $\alpha=2.5$  exactly, whereas  $\alpha>2.5$  and  $\alpha<2.5$  for repulsive and attractive loop interactions, respectively [33]. Unfortunately, we cannot distinguish among these three possibilities in our data.

While the relative depths of the wells appearing in the histogram Fig. 1 are sensitive to temperature variations as small as 0.0001 about  $T_{NI}$ , the distribution  $D(p)$  is less sensitive. A plot of  $D(p)$  at  $T=1.1225$ , e.g., would be qualitatively similar to the appearance of  $D(p)$  at  $T_{NI}$ , the upper curve in Fig. 2. However, deeper in the nematic phase at  $T=1.120$  (where the isotropic free energy well has disappeared) and  $T=1.10$ , the behavior of  $D(p)$  is different. Here, one can clearly see an exponential decay at large values of  $p$  and the data can be fit to the form given in Eq. (3) with line tensions 0.003 and 0.026 at  $T=1.120$  and 1.10, respectively (these values were computed setting  $\alpha=2.5$ ).

The behavior of  $D(p)$  shown in Fig. 2 is consistent with a “blowout” of disclination loops at the NI transition, similar to the behavior found in the three-dimensional  $XY$  model [11]. However, as indicated in the previous paragraph,  $D(p)$  provides a less sensitive measure of the transition temperature compared to the histogram of the disclination line segments. The source of this drawback is the appearance of the bump at large perimeters in  $D(p)$  in the neighborhood of  $T_{NI}$  which is a finite-size effect, arising from the nonzero probability of forming loops that wrap completely around the lattice due to the periodic boundary conditions. At high enough temperatures (in particular, near the transition and above) there will be a sufficient number of disclination line segments present to form such loops. The value of  $\alpha$  for these loops is predicted to be unity for noninteracting loops in three dimensions [34]. The crossover in  $D(p)$  from infinite system behavior (with  $\alpha \approx 2.5$ ) to the finite system behavior is expected to occur at a critical perimeter  $p_c(L) \approx 1.5L^2/\pi$  for a system of size  $L$  [34]. Our results are in very good agreement with this scenario as shown in Fig. 2. The

truncation of  $D(p)$  at very large perimeters occurs because there are not enough disclination line segments (since we eliminated the previously marked ones) to construct loops with arbitrarily large perimeters. The deviation from the expected  $\alpha=2.5$  behavior for small  $p$  is due to the presence of the underlying lattice structure of the LL model.

We attempted to measure the jump in the effective line tension  $\epsilon$  at  $T_{NI}$  in the LL model which is expected to occur because of the first-order nature of the NI transition, in contrast to the continuous vanishing of  $\epsilon$  observed in the XY model [11]. Naively, one should compute  $D(p)$  for temperatures in the vicinity of  $T_{NI}$  and extract the line tension  $\epsilon(T)$  using Eq. (3) to fit the data. However, in practice, this procedure is very difficult to carry out because the NI transition is weakly first order in the LL model and the jump in  $\epsilon$  must be determined from the behavior of loops with very large perimeters. But loops with large perimeters wrap around the lattice as we described in the previous paragraph and thus appear in the “bump” region of Fig. 2 that cannot be fit with Eq. (3).

Another possibility would be to set the temperature to a value close to  $T_{NI}$ , calculate the nematic order parameter, and then compute  $D(p)$  separately in the isotropic and nematic phases. In principle, the difference between the two distributions should give the jump in  $\epsilon$  at the given temperature. However, again due to the very weak first-order nature of the transition we found that each of these distributions was qualitatively similar to the critical distribution shown in Fig. 2. Thus, at least for the systems sizes we have been able to study (less than or equal to  $70^3$ ), we have found it impossible to accurately measure the expected jump in the disclination line tension in the LL model.

To check our supposition that the disclination line tension should have a discontinuous jump at the first-order NI transition, we considered a modified LL model, including a fourth-order Legendre polynomial  $P_4$ , which has been shown to make the NI transition more strongly first order [26,35]. The modified Hamiltonian is given by

$$\mathcal{H}' = -J \sum_{\langle ij \rangle} P_2(\sigma_i \cdot \sigma_j) - J' \sum_{\langle ij \rangle} P_4(\sigma_i \cdot \sigma_j). \quad (4)$$

This modified LL model was studied in Ref. [26] for a system of size  $24^3$  with  $J'/J=0.1$ . We checked that the cluster algorithm produces free energy plots similar to those obtained in the latter reference where the single flip Monte Carlo algorithm was used.

We were able to measure the jump in the line tension for a system of size  $50^3$  with  $J'/J=0.3$  as shown in Fig. 3, finding a jump of approximately 0.0024 at the transition temperature  $T=1.2475$ . Here, we calculated  $D(p)$  separately in the isotropic and nematic phases, with a production run of  $10^7$  MCS. We have been unable to carry out a finite-size scaling analysis of the jump because one has to choose the ratio  $J'/J$  large enough so that  $D(p)$  exhibits behavior consistent with the form of Eq. (3) at large  $p$  in nematic phase; in particular with no “bump” as in Fig. 2. However, this choice of  $J'/J$  makes the transition more strongly first order and large systems can hardly overcome the resulting large free-

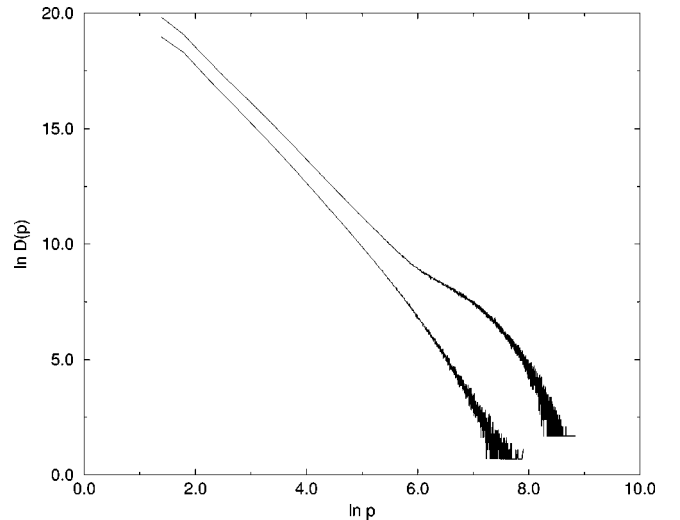


FIG. 3. Log-log plot of the disclination loop distribution function  $D(p)$  for the modified Lebwohl-Lasher model, Eq. (4), at its NI transition temperature  $T=1.2475$ . The system size is  $50^3$  and the ratio of the couplings is  $J'/J=0.3$ . The top curve (which has been displaced for the sake of clarity) and the bottom curve correspond to the isotropic and nematic wells of the free energy, respectively. The jump in the disclination line tension is found to be 0.0024, and the straight portion of the isotropic data can be fit with a power law of  $2.50 \pm 0.01$  [see Eq. (3)].

energy barrier. We also measured a histogram of the density of disclination line segments for the modified model and found behavior similar to that found in the LL model (see Fig. 1), namely equal well depths for this quantity at the *same* temperature where the free energy also exhibits two wells of equal depth.

As we discussed in Sec. I, topological defects in nematics include not only disclination loops but monopoles as well, and furthermore, the disclination loops can potentially carry monopole charge. To locate monopoles, we used the prescription introduced by Berg and Lüscher [36] for the two-dimensional Heisenberg model that was subsequently extended by Lau and Dasgupta [12] to three dimensions. Each of the six faces of a lattice cube is divided into two equal area triangles by the face diagonal. The rotors  $\sigma_1$ ,  $\sigma_2$ , and  $\sigma_3$  at the three corners of each of the triangles are mapped to points on the order-parameter sphere, forming spherical triangles. The area of each of the twelve spherical triangles formed by this mapping is then computed, with a sign given by  $\text{sgn}[\sigma_1 \cdot (\sigma_2 \times \sigma_3)]$ . The rotors on each triangle are numbered so that the circuit  $1 \rightarrow 2 \rightarrow 3 \rightarrow 1$  corresponds to a counterclockwise rotation along the outward normal to the surface of the triangle. In performing this mapping, we have assigned heads to the rotors such that the distance between the heads on the order-parameter sphere is minimized, i.e., we use the “geodesic rule” [37–39] to effectively minimize the energy. For lattice cubes that are not pierced by disclination lines (and it is these cubes that we examine for monopole charge), the heads of all eight rotors at the corners of a cube can be simultaneously chosen to obey the geodesic rule without frustration. Thus, the angle between any pair of rotors at the corners of any of the twelve triangles will be no



greater than  $90^\circ$ . Finally, the monopole charge enclosed by the cube is given by the sum of the twelve signed areas of the spherical triangles, divided by  $4\pi$ .

Using this algorithm, we examined all lattice cubes that are not pierced by disclination lines and found *no* monopoles, neither in the original LL model, Eq. (1), nor the modified model, Eq. (4). We searched for monopoles in the neighborhood of  $T_{NI}$ , deep in the nematic phase and at very high temperatures; in all cases, no monopoles were located. This null result is not surprising given the topological arguments advanced by Hindmarsh [40] which yield a very low probability (of order  $10^{-8}$ , compared with  $1/8$  for the Heisenberg model) for the appearance of point monopoles in a nematic.

One way to measure the monopole charge of a disclination loop would be to apply the above algorithm to the surface of a group of lattice cubes that completely enclose a disclination loop. We have carried out this procedure for isolated loops of perimeter  $p=4$ ; none of these loops were found to carry monopole charge. It is difficult to carry out this procedure for larger loops, especially when two or more loops are entangled. In particular, when loops are entangled, it is impossible to impose the geodesic rule simultaneously on all pairs of rotors. If we surround one loop completely with a set of lattice cubes, frustration will arise where the second loop pierces one of these lattice cubes. Instead, we measured the local rotation vector  $\mathbf{\Omega}$  of the four rotors surrounding each of the segments that form a disclination loop, and then summed these vectors along the entire length of the loop. If this sum is nearly zero, then the loop carries a non-zero monopole charge, because the set of rotors surrounding the entire loop will cover essentially the entire order-parameter sphere [42,43]. A simple example of this topology occurs in the case of a pure wedge loop where  $\mathbf{\Omega}$  is everywhere tangent to the loop [41], and summing this vector around the loop yields zero identically; a simple example of a loop with zero monopole charge is a twist loop where  $\mathbf{\Omega}$  is everywhere perpendicular to the plane of the loop. We measured the local rotation vector  $\mathbf{\Omega}$  of the four rotors  $\sigma_1, \sigma_2, \sigma_3, \sigma_4$  that lie at the corners of a lattice square pierced by a disclination line, by summing the vector cross product of each neighboring pair of rotors [44]:

$$\mathbf{\Omega} = (\sigma_1 \times \sigma_2) + (\sigma_2 \times \sigma_3) + (\sigma_3 \times \sigma_4) + [\sigma_4 \times (-\sigma_1)]. \quad (5)$$

In writing this definition of  $\mathbf{\Omega}$ , we have chosen the heads of the rotors so that the neighboring pairs  $\sigma_1, \sigma_2$ ;  $\sigma_2, \sigma_3$ , and  $\sigma_3, \sigma_4$  satisfy the ‘‘geodesic rule’’ on the order-parameter sphere. The remaining pair  $\sigma_4, \sigma_1$  will not satisfy this rule because of the presence of the disclination line segment; thus we reflect  $\sigma_1$  in the last term in Eq. (5), so that the vector products always involve pairs of rotors that satisfy the geodesic rule. To assign a unique sense to the circuit  $1 \rightarrow 2 \rightarrow 3 \rightarrow 4 \rightarrow 1$ , we arbitrarily assign a direction along the length of the disclination loop, and traverse the circuit in a counterclockwise sense along this direction. We note that the reflection of  $\sigma_1$  in the last term of Eq. (5) guarantees that  $\mathbf{\Omega}$  is independent of which of the four rotors is labeled one.

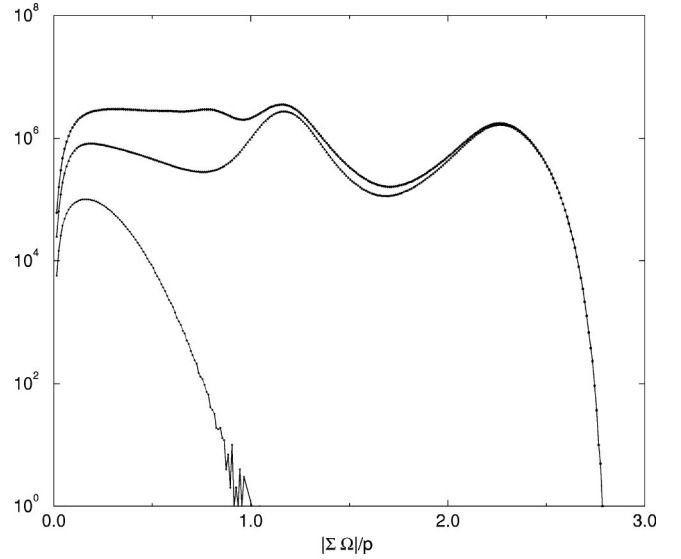


FIG. 4. The distribution of  $|\Sigma\mathbf{\Omega}|/p$ , the magnitude of the vector sum of the rotation vector  $\mathbf{\Omega}$ , Eq. (5), along each disclination loop divided by its perimeter  $p$ , in the LL model of size  $50^3$  at  $T_{NI}$ . The top curve includes loops of all perimeters, the middle curve includes loops of  $p=4$  only, while the bottom curve includes only loops with  $p>100$ . The rightmost peak appearing in the middle curve corresponds to isolated loops. Note that for a perfect wedge line segment piercing a square face of a lattice cube [i.e., a rotor configuration of the form  $\sigma = (\cos \phi/2, \sin \phi/2)$ , where  $\phi$  is the azimuthal angle of the lattice site],  $|\Sigma\mathbf{\Omega}|$  is given by  $2\sqrt{2} \approx 2.8$ .

Our results for the vector sum of  $\mathbf{\Omega}$  along each disclination loop are shown in Fig. 4 for the LL model at its NI transition temperature  $T_{NI} = 1.12279$  for a system of size  $50^3$ . We use a smaller system size because the computation of this vector sum must be done using scalar code, whereas the cluster algorithm used above can be vectorized [30]. Similar results were obtained for the modified LL model. We note that all of the large loops with perimeters  $p \geq 100$  are characterized by net rotation vectors that are nearly zero, suggesting that they carry nonzero monopole charge. We expect on energetic grounds that this charge will be unity rather than higher values. We have checked this supposition for a random sampling of loops finding that the rotation vectors cover a great circle on the order-parameter sphere just once. Our data indicates that small isolated loops do not carry monopole charge. Rather the monopole charge is carried by large loops (with perimeters greater than 100) and small loops that touch larger ones.

### III. CONCLUSIONS

In this paper, we have studied the properties of topological defects in two lattice models of the NI transition: the original Lebwohl-Lasher model (which exhibits a weakly first-order transition) and a modified model with a more strongly first-order transition. We have found evidence for the role played by disclination loops at the NI transition in both models. Namely, a histogram of disclination line segments collected over the course of the MC simulation shows a double-well structure, and the wells are of equal depth at

the *same* temperature where the free energy exhibits similar structure. We also find that the distribution  $D(p)$  of disclination loops as a function of their perimeter exhibits power-law behavior at this temperature, consistent with the “blowout” of loops at the transition. However,  $D(p)$  is a less sensitive measure of the transition temperature compared with the disclination segment histogram, due to finite-size effects.

We have also searched for point monopoles in these models and measured the monopole charge of the disclination loops. We found no point monopoles, a result that may be reasonable on the basis of topological arguments [40]. However, we did find that nearly all of the large disclination loops carry monopole charge, while small isolated loops do not. Of particular interest is the result that the two models we studied, one with a weakly first-order transition and the other with a strongly first-order transition, showed no qualitative differences in their defect characteristics, other than the measurable jump in the disclination line tension in the latter model. In light of the results of Ref. [19] we find the similarities in the defect characteristics of the models we studied somewhat surprising. In Ref. [19], it was shown that suppressing disclination loops while leaving monopoles yields a more continuous NI transition. One might guess then that moving in the opposite direction to a model like that given in

Eq. (4) which exhibits a strongly first-order transition one would find fewer monopolelike entities than in the LL model with its weakly first-order transition. While neither model has point monopoles, both appear to have similar densities of disclination loops with monopole charge, suggesting that monopole charge may not influence the strength of the first-order transition. We should also note that while our results suggest that disclination loops “blowout” at the NI transition in both models we considered, it is not clear from our study whether the transition is in fact defect driven, or rather that some other mechanism drives the transition and the defects simply respond. Clearly, more work on this very intriguing phase transition and the role played by topological defects would be of considerable interest.

#### ACKNOWLEDGMENTS

We thank A. Sudbó, J. M. Kosterlitz, and J. Toner for numerous helpful discussions. This work was supported by the National Science Foundation under Grant No. DMR-9873849. Computational work in support of this research was performed at Brown University’s Theoretical Physics Computing Facility.

- 
- [1] J. M. Kosterlitz and D. J. Thouless, *J. Phys. C* **6**, 1181 (1973).  
 [2] J. M. Kosterlitz, *J. Phys. C* **7**, 1046 (1974).  
 [3] D. R. Nelson and B. I. Halperin, *Phys. Rev. B* **19**, 2457 (1979).  
 [4] A. P. Young, *Phys. Rev. B* **19**, 1855 (1979).  
 [5] J. Villain, *J. Phys. (Paris)* **36**, 581 (1975).  
 [6] R. Savit, *Phys. Rev. B* **17**, 1340 (1978).  
 [7] L. Onsager, *Nuovo Cimento, Suppl.* **6**, 249 (1949).  
 [8] R. P. Feynman, in *Progress in Low Temperature Physics*, edited by C. J. Gorter (North-Holland, Amsterdam, 1955), Vol. 1, p. 17.  
 [9] B. Chattopadhyay, M. C. Mahato, and S. R. Shenoy, *Phys. Rev. B* **47**, 15 159 (1993); G. A. Williams, *Phys. Rev. Lett.* **82**, 1201 (1999).  
 [10] G. Kohring, R. E. Shrock, and P. Wills, *Phys. Rev. Lett.* **57**, 1358 (1986).  
 [11] A. K. Nguyen and A. Sudbó, *Phys. Rev. B* **57**, 3123 (1998); **60**, 15 307 (1999).  
 [12] M. H. Lau and C. Dasgupta, *Phys. Rev. B* **39**, 7212 (1989).  
 [13] C. Holm and W. Janke, *J. Phys. A* **27**, 2553 (1994).  
 [14] P. de Gennes and J. Prost, *The Physics of Liquid Crystals* (Clarendon Press, Oxford, 1993).  
 [15] While monopoles in nematics are characterized by the absolute value of the integer charge, when monopoles with charges  $n$  and  $m$  coalesce, the resulting singularity can have charge of either  $|n|+|m|$  or  $||n|-|m||$  depending on the coalescence process; see G. E. Volovik and V. P. Mineev, *Zh. Éksp. Teor. Fiz.* **72**, 2256 (1977) [*Sov. Phys. JETP* **45**, 1186 (1978)].  
 [16] N. D. Mermin, *Rev. Mod. Phys.* **51**, 591 (1979).  
 [17] R. B. Meyer, *Philos. Mag.* **27**, 405 (1973).  
 [18] A. T. Garel, *J. Phys. (Paris)* **39**, 225 (1978); V. P. Mineev, *Sov. Sci. Rev., Sect. A* **2**, 173 (1980); H. Nakanishi, K. Hayashi, and H. Mori, *Commun. Math. Phys.* **117**, 203 (1988); H. Mori and H. Nakanishi, *J. Phys. Soc. Jpn.* **57**, 1281 (1988).  
 [19] P. E. Lammert, D. S. Rokhsar, and J. Toner, *Phys. Rev. Lett.* **70**, 1650 (1993); *Phys. Rev. E* **52**, 1778 (1995); J. Toner, P. E. Lammert, and D. S. Rokhsar, *ibid.* **52**, 1801 (1995).  
 [20] P. A. Lebowitz and G. Lasher, *Phys. Rev. A* **47**, 4780 (1972).  
 [21] G. R. Luckhurst and P. Simpson, *Mol. Phys.* **47**, 251 (1982).  
 [22] U. Fabbri and C. Zannoni, *Mol. Phys.* **4**, 763 (1986).  
 [23] C. Zannoni, *J. Chem. Phys.* **84**, 424 (1986).  
 [24] G. Kohring and R. E. Shrock, *Nucl. Phys. B* **285**, 504 (1987).  
 [25] F. Biscarini, C. Zannoni, C. Chiccoli, and P. Pasini, *Mol. Phys.* **73**, 439 (1991).  
 [26] Z. Zhang, O. G. Mouritsen, and M. J. Zuckermann, *Phys. Rev. Lett.* **69**, 2803 (1992); Z. Zhang, M. J. Zuckermann, and O. G. Mouritsen, *Mol. Phys.* **80**, 1195 (1993).  
 [27] S. Boschi, M. P. Brunelli, C. Zannoni, C. Chiccoli, and P. Pasini, *Int. J. Mod. Phys. C* **8**, 547 (1997).  
 [28] H. Kunz and G. Zumbach, *Phys. Lett. B* **257**, 299 (1991); *Phys. Rev. B* **46**, 662 (1992). See also, S. Caracciolo, R. G. Edwards, A. Pelissetto, and A. D. Sokal, *Nucl. Phys. B* **403**, 475 (1993).  
 [29] U. Wolff, *Phys. Rev. Lett.* **62**, 361 (1989).  
 [30] N. V. Priezjev and R. A. Pelcovits, *Phys. Rev. E* **63**, 062702 (2001).  
 [31] A. M. Ferrenberg and R. H. Swendsen, *Phys. Rev. Lett.* **61**, 2635 (1988).  
 [32] M. Zapotocky, P. M. Goldbart, and N. Goldenfeld, *Phys. Rev. E* **51**, 1216 (1995).  
 [33] N. D. Antunes and L. M. A. Bettencourt, *Phys. Rev. Lett.* **81**, 3083 (1998).  
 [34] D. Austin, E. J. Copeland, and R. J. Rivers, *Phys. Rev. D* **49**, 4089 (1994).

- [35] C. Zannoni, *Mol. Cryst. Liq. Cryst.* **49**, 247 (1979); C. Chiccoli, P. Pasini, P. Biscarini, and C. Zannoni, *Mol. Phys.* **65**, 1505 (1988); C. Chiccoli, P. Pasini, and C. Zannoni, *Int. J. Mod. Phys. B* **11**, 1937 (1997).
- [36] B. Berg and M. Lüscher, *Nucl. Phys. B* **190**, 412 (1981).
- [37] T. Vachaspati, *Phys. Rev. D* **44**, 3723 (1991).
- [38] S. Rudaz and A. M. Srivastava, *Mod. Phys. Lett. A* **8**, 1443 (1993).
- [39] M. Hindmarsh, A.-C. Davis, and R. Brandenberger, *Phys. Rev. D* **49**, 1944 (1994).
- [40] M. Hindmarsh, *Phys. Rev. Lett.* **75**, 2502 (1995).
- [41] A. H. Windle, H. E. Assender, and M. S. Lavine, *Proc. R. Soc. London, Ser. A* **348**, 73 (1994).
- [42] E. M. Terentjev, *Phys. Rev. E* **51**, 1330 (1995).
- [43] M. Zapotocky and T. C. Lubensky (unpublished).
- [44] J. Hobdell and A. Windle, *Liq. Cryst.* **23**, 157 (1997).